the impedance bandwidth increases with an increasing value of R_F. It is also observed that two resonant modes are excited, owing to the broadband characteristics of the passive slotted triangular microstrip antenna [3]. The impedance bandwidth, determined from the 10 dB return loss, for the case with $R_F = 50.7$ kΩ, is as large as 164 MHz or about 9.3% referenced to the center frequency at 1760 MHz. (The center frequency is defined here to be the frequency $(f_L + f_H)/2$, where f_L and f_H are the lower and higher frequencies with 10 dB return loss in the impedance bandwidth.) This impedance bandwidth is about 2.0 times that of the passive slotted antenna studied here (about 4.7% [3]) or 6.0 times that of the passive simple triangular microstrip antenna without slots (about 1.6%). The obtained impedance bandwidths of the other two cases with $R_F = 33.3$ and 42.7 kΩ are also larger than that of the passive slotted antenna, and are 125 MHz (about 7.1%) and 135 MHz (about 7.6%), respectively.

The radiation characteristics and antenna gain are also studied. Figure 3 shows the typical measured E-plane (y–z plane) and H-plane (x–z plane) radiation patterns at the two resonant modes of the active antenna with $R_F = 50.7$ kΩ. The obtained results show good radiation characteristics. Figure 4 presents the measured antenna gain in the broadside direction against frequency for the active antennas studied in Figure 2. Results clearly indicate that the antenna

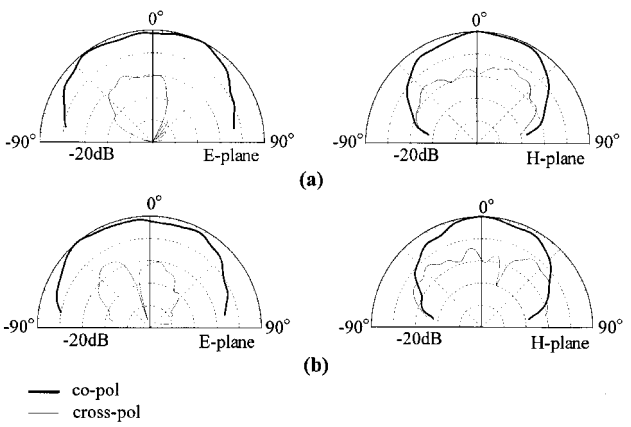

Figure 3 Measured E-plane (y–z plane) and H-plane (x–z plane) radiation patterns of the active antenna studied in Figure 2 with $R_F = 50.7$ kΩ. (a) $f = 1752$ MHz. (b) $f = 1808$ MHz

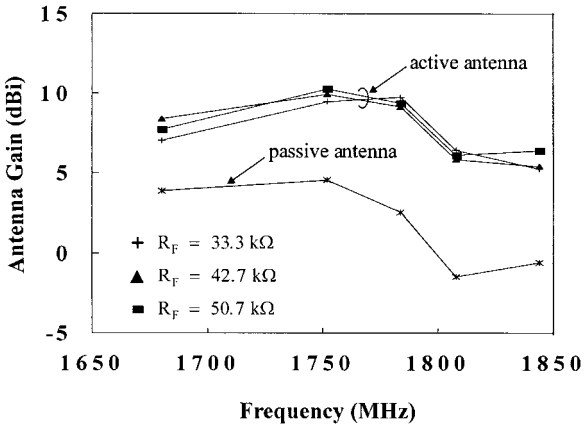

Figure 4 Measured antenna gain in the broadside direction against frequency for the active antennas studied in Figure 2

gains of the active antennas with various bias feedback resistances are about the same, and are about 6 dB greater than that of the passive slotted triangular microstrip antenna. Also, relatively more uniformity in the antenna gain as a function of frequency is observed for the active antennas, as compared to that of the passive slotted triangular microstrip antenna shown in the figure.

4. CONCLUSIONS

An amplifier-type active microstrip antenna, as a transmitting antenna, with enhanced gain and bandwidth has been implemented and studied. It is shown that, with the selection of a possible maximum feedback resistance in the active circuitry, the impedance bandwidth of the active antenna can be greatly enhanced for a given extra output gain. For the specific design studied here, the obtained impedance bandwidth can be as large as two times that of the passive slotted microstrip antenna or six times that of the passive conventional unslotted triangular microstrip antenna.

REFERENCES

1. J. Lin and T. Itoh, Active integrated antennas, IEEE Trans Microwave Theory Tech 42 (1994), 2186–2194.
2. B. Robert, T. Razban, and A. Papiernik, Compact amplifier integration in square patch antenna, Electron Lett 28 (1992), 1808–1810.
3. S.T. Fang, K.L. Wong, and T.W. Chiou, Bandwidth enhancement of inset-microstrip-line-fed equilateral-triangular microstrip antenna, Electron Lett 34 (1998), 2184–2186.

CCC 0895-2477/99

FAST FREQUENCY-SWEEP ANALYSIS OF CAVITY-BACKED MICROSTRIP PATCH ANTENNAS

Dan Jiao[1] and Jian-Ming Jin[1]
[1] Center for Computational Electromagnetics
Department of Electrical and Computer Engineering
University of Illinois at Urbana – Champaign
Urbana, Illinois 61801-2991

Received 15 March 1999

ABSTRACT: *A fast frequency-sweep technique is presented for the analysis of cavity-backed microstrip patch antennas. This technique applies the method of asymptotic waveform evaluation (AWE) to the hybrid finite-element boundary-integral (FE–BI) solution of the original boundary-value problem. Numerical examples show that the proposed technique can speed up the analysis by more than an order of magnitude.* © 1999 John Wiley & Sons, Inc. Microwave Opt Technol Lett 22: 389–393, 1999.

Key words: *asymptotic waveform evaluation; finite-element method; microstrip antennas*

I. INTRODUCTION

Since microstrip patch antennas are resonant structures, their characteristics, such as input impedance, vary drastically as a function of frequency. As a result, when a microstrip patch antenna is analyzed using a frequency-domain-based method, the analysis must be repeated many times with a small frequency increment in order to obtain its response over a frequency band. This often leads to excessive computing time,

especially when many design variations have to be evaluated. In this letter, we present a numerical procedure to alleviate this difficulty. In this procedure, we apply the method of asymptotic waveform evaluation (AWE) to the hybrid finite-element boundary-integral (FE–BI) solution of scattering and radiation from a cavity-backed microstrip patch antenna. Our numerical examples show that the proposed technique can speed up the analysis by more than an order of magnitude.

II. FORMULATION

The FE–BI method is a powerful numerical technique for solving electromagnetic scattering and radiation problems [1–3]. This technique divides an open-region problem into interior and exterior problems, and employs the finite-element method to deal with the interior problem. The exterior problem is formulated using the boundary-integral method which, when coupled with interior fields, provides an efficient solution to the original problem.

For the problem of scattering and radiation by a cavity-backed microstrip patch antenna recessed in a ground plane (Fig. 1), it has been shown [3] that the electric field inside the cavity and over the aperture can be found by seeking the stationary point of the functional

$$\begin{aligned} F(\mathbf{E}) = {} & \frac{1}{2}\iiint_V \left[\frac{1}{\mu_r}(\nabla\times\mathbf{E})\cdot(\nabla\times\mathbf{E}) - k^2\epsilon_r\mathbf{E}\cdot\mathbf{E}\right] dV \\ & + \iiint_V \left[jkZ\mathbf{J}^{\text{int}}\cdot\mathbf{E} - \frac{1}{\mu_r}\mathbf{M}^{\text{int}}\cdot(\nabla\times\mathbf{E})\right] dV \\ & - k^2\iiint_S \mathbf{M}(\mathbf{r})\cdot\left[\iint_S \mathbf{M}(\mathbf{r}')G(\mathbf{r},\mathbf{r}')\,dS'\right] dS \\ & + \iint_S \nabla\cdot\mathbf{M}(\mathbf{r})\left[\iint_S G(\mathbf{r},\mathbf{r}')\nabla'\cdot\mathbf{M}(\mathbf{r}')\,dS'\right] dS \\ & - 2jkZ\iint_S \mathbf{M}(\mathbf{r})\cdot\mathbf{H}^{\text{inc}}(\mathbf{r})\,dS \end{aligned} \tag{1}$$

where V denotes the volume of the cavity and S denotes its aperture, $\mathbf{M} = \mathbf{M}\times\hat{z}$ is the equivalent magnetic current over the aperture, k is the free-space wavenumber, Z is the free-space wave impedance, and $G(\mathbf{r},\mathbf{r}')$ denotes the free-space Green's function:

$$G(\mathbf{r},\mathbf{r}') = \frac{e^{-jk|\mathbf{r}-\mathbf{r}'|}}{4\pi|\mathbf{r}-\mathbf{r}'|}. \tag{2}$$

For scattering problems, $\mathbf{H}^{\text{inc}}$ denotes the incident magnetic field. For radiation problems, $\mathbf{J}^{\text{int}}$ and $\mathbf{M}^{\text{int}}$ denote the electric and magnetic sources associated with the antenna feeds.

The discretization of the above functional has been described in detail in the past [3]. It leads to the matrix equation

$$A(k)E(k) = B(k) \tag{3}$$

where A is a partly sparse and partly full symmetric matrix, E is a vector representing the discretized electric field, and B is the excitation vector related to the incident field for scattering or internal sources for radiation.

Since the matrix A in (3) depends on frequency, it must be generated and solved repeatedly at each individual frequency in order to obtain a solution over a frequency band. This can be time consuming, especially for microstrip patch antennas whose response varies drastically with frequency. In this work, we alleviate this problem using the AWE method.

The AWE method was originally developed for high-speed circuit analysis [4, 5]. In AWE, the transfer function of a circuit is expanded into a series, and the circuit model is then approximated with a lower order transfer function by moment matching. This method has recently been applied to the finite-element and finite-difference analysis of electromagnetics problems [6–13]. It has also been applied to the method-of-moments solution of scattering [14–16] and microstrip structures in a multilayered medium [17].

In accordance with the AWE method, to obtain the solution of (3) over a wide frequency band, we expand $E(k)$ into a Taylor series:

$$E(k) = \sum_{n=0}^{Q} m_n(k-k_0)^n \tag{4}$$

where k_0 is the expansion point. Substituting this into (3), expanding the impedance matrix $A(k)$ and the excitation vector $B(k)$ into a Taylor series, and finally matching the coefficients of the equal powers of $k-k_0$ on both sides yield the recursive relation for the moment vectors:

$$m_0 = A^{(-1)}(k_0)B(k_0) \tag{5}$$

$$m_n = A^{(-1)}(k_0)\left[\frac{B^{(n)}(k_0)}{n!} - \sum_{i=1}^{n}\frac{A^{(i)}(k_0)m_{n-i}}{i!}\right], \qquad n \geq 1 \tag{6}$$

where $A^{(-1)}$ denotes the inverse of A, $A^{(i)}$ denotes the ith derivative of A, and likewise, $B^{(n)}$ denotes the nth derivative of B. These derivatives are found analytically in this work.

The Taylor expansion has a limited bandwidth. To obtain a wider bandwidth, we represent $E(k)$ with a better behaved rational Padé function:

$$E(k) = \frac{\sum_{i=0}^{L} a_i(k-k_0)^i}{1+\sum_{j=1}^{M} b_j(k-k_0)^j} \tag{7}$$

where $L+M=Q$. The unknown coefficients a_i and b_j can be calculated by substituting (4) into (7), multiplying (7) with the denominator of the Padé expansion, and matching the

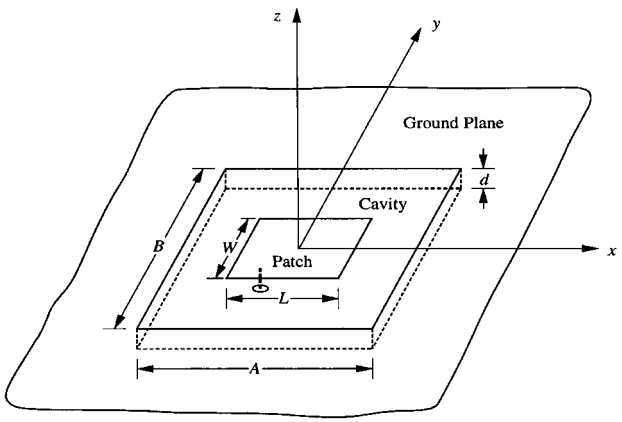

Figure 1 Illustration of a cavity-backed microstrip patch antenna

coefficients of the equal powers of $k - k_0$. This leads to the matrix equation

$$\begin{bmatrix} m_L & m_{L-1} & m_{L-2} & \cdots & m_{L-M+1} \\ m_{L+1} & m_L & m_{L-1} & \cdots & m_{L-M+2} \\ m_{L+2} & m_{L+1} & m_L & \cdots & m_{L-M+3} \\ \vdots & \vdots & \vdots & \ddots & \vdots \\ m_{L+M-1} & m_{L+M-2} & m_{L+M-3} & \cdots & m_L \end{bmatrix} \times \begin{bmatrix} b_1 \\ b_2 \\ b_3 \\ \vdots \\ b_M \end{bmatrix} = - \begin{bmatrix} m_{L+1} \\ m_{L+2} \\ m_{L+3} \\ \vdots \\ m_{L+M} \end{bmatrix} \quad (8)$$

which can be solved for b_j. Once b_j are obtained, the unknown coefficients a_i can then be calculated as

$$a_i = \sum_{j=0}^{i} b_j m_{i-j}, \qquad 0 \le i \le L. \quad (9)$$

Clearly, in the procedure described above, the impedance matrix $A(k)$ is inverted only once, which is the main reason for the efficiency of the AWE method. In the case where one expansion point is not sufficient to cover the desired frequency band, one can use multipole expansion points, which can be selected automatically using a simple binary search algorithm [7, 11].

III. NUMERICAL EXAMPLES

To demonstrate the efficiency and accuracy of the proposed method, a number of numerical examples are considered.

The first example is scattering by an antenna geometry consisting of a 3.66 cm × 2.60 cm rectangular conducting patch residing on a dielectric substrate having thickness t = 0.158 cm, relative permittivity $\epsilon_r = 2.17$, and a loss tangent of 0.001. The substrate is housed in a 7.32 cm × 5.20 cm rectangular cavity recessed in a ground plane. The incident plane wave is polarized along the $\hat{\theta}$-direction, and the angle of incidence is $\theta^{\text{inc}} = 60°$ and $\phi^{\text{inc}} = 45°$. The monostatic radar cross section (RCS) of the antenna is shown in Figure 2 as a function of frequency from 2 to 8 GHz. Clearly, the RCS is characterized by a series of peaks, each corresponding to a resonant mode of the patch. The results compare well with the experimental data for the patch residing on an infinite substrate [18].

The number of unknowns used in the calculation is 1585. With a frequency increment of 0.05 GHz, it takes the direct method, which solves (2) repeatedly for each frequency, 3254.4 s to obtain the solution on a digital personal workstation (500 MHz Alpha 21164 processor). With a sixth-order Taylor expansion ($Q = 6$, $L = 3$, $M = 3$), the AWE method produces an accurate solution with 0.01 GHz increments over the entire band in 265.2 s.

The second example is radiation by an antenna geometry consisting of a 5.0 cm × 3.4 cm rectangular conducting patch residing on a dielectric substrate having thickness t = 0.08770 cm, relative permittivity $\epsilon_r = 2.17$, and a loss tangent of 0.0015. The substrate is housed in a 7.5 cm × 5.1 cm rectangular cavity recessed in a ground plane. The patch is excited by a current probe applied at x_f = 1.22 cm and y_f = 0.85 cm.

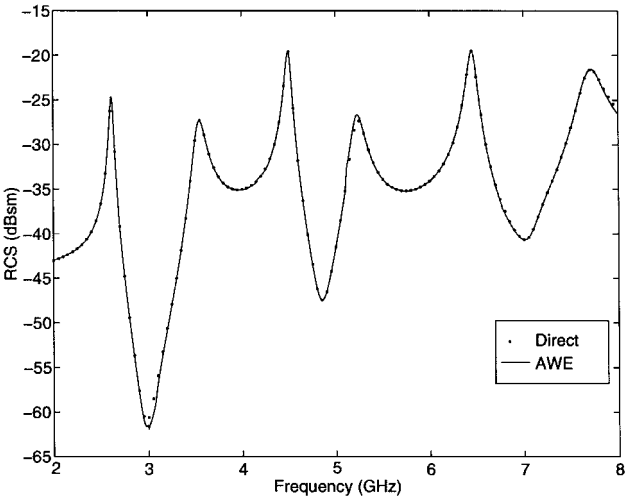

Figure 2 Monostatic VV-polarized RCS versus frequency for a cavity-backed patch antenna (A = 7.32 cm, B = 5.20 cm, L = 3.66 cm, W = 2.60 cm, d = 0.158 cm, $\epsilon_r = 2.17$, tan δ = 0.001, $\theta^{\text{inc}} = 60°$, $\phi^{\text{inc}} = 45°$)

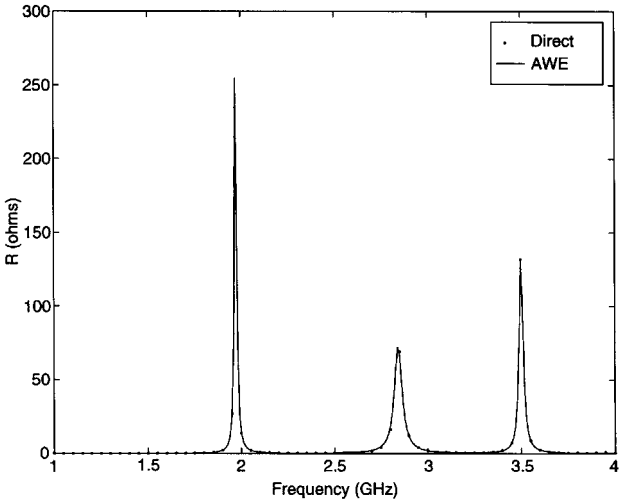

(a)

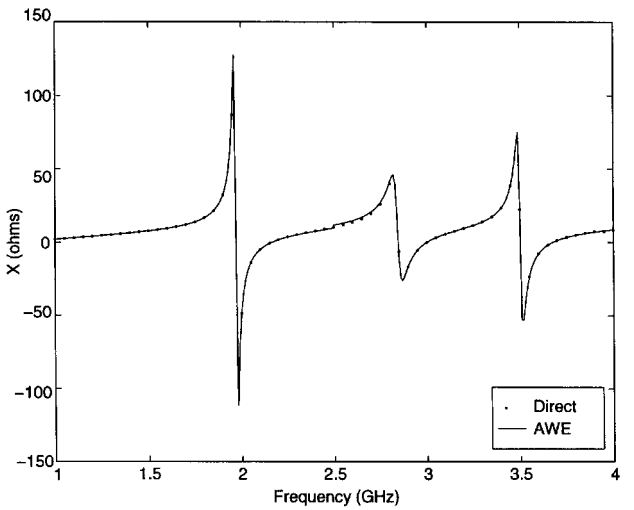

(b)

Figure 3 Input impedance versus frequency for a cavity-backed patch antenna with a probe feed at x_f = 1.22 cm and y_f = 0.85 cm (A = 7.5 cm, B = 5.1 cm, L = 5.0 cm, W = 3.4 cm, d = 0.08779 cm, $\epsilon_r = 2.17$, tan δ = 0.0015). (a) Resistance. (b) Reactance

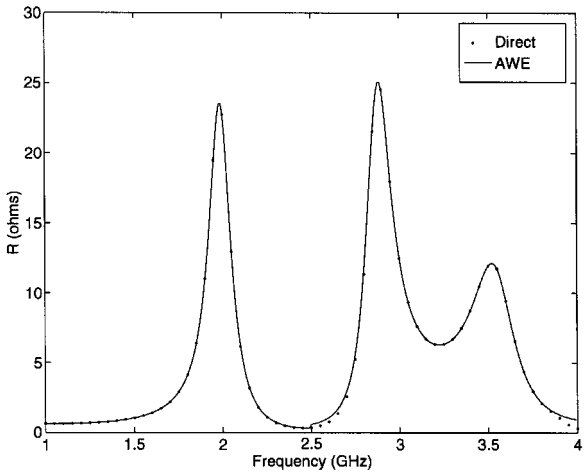

Figure 4 Input impedance versus frequency for a cavity-backed patch antenna with a probe feed at $x_f = 1.22$ cm and $y_f = 0.85$ cm and a 50 Ω resistor load at $x_L = -2.2$ cm and $y_L = -1.5$ cm ($A = 7.5$ cm, $B = 5.1$ cm, $L = 5.0$ cm, $W = 3.4$ cm, $d = 0.08779$ cm, $\epsilon_r = 2.17$, $\tan\delta = 0.0015$). (a) Resistance. (b) Reactance

Figure 3 shows the input impedance of the antenna as a function of frequency from 1 to 4 GHz. Figure 4 shows the input impedance when a 50 Ω impedance load is placed at $x_L = -2.2$ cm and $y_L = -1.5$ cm. The calculated results compare well with the experimental data for the patch residing on an infinite substrate [18].

The number of unknowns used in the calculations is 1741. With a frequency increment of 0.05 GHz, it takes the direct method 4012.8 s to obtain the solution. With a sixth-order Taylor expansion ($Q = 6$, $L = 3$, $M = 3$), the AWE method produces an accurate solution with 0.01 GHz increments over the entire band in 254.2 s.

The information on the calculations is summarized in Table 1 for a clear comparison. In both cases, the speed-up is more than an order of magnitude.

IV. CONCLUSION

A fast frequency-sweep technique is described for the analysis of cavity-backed microstrip patch antennas. This technique applies the AWE method to the FE–BI solution of the original boundary-value problem. Numerical examples show that the proposed technique can speed up the analysis by more than an order of magnitude.

ACKNOWLEDGMENT

This work was supported by the National Science Foundation number Grant NSF ECE 94-57735.

REFERENCES

1. J.M. Jin, J.L. Volakis, and J.D. Collins, A finite element-boundary integral method for scattering and radiation by two- and three-dimensional structures, IEEE Antennas Propagat Mag 33 (1991), 22–32.
2. J.M. Jin and J.L. Volakis, A hybrid finite element method for scattering and radiation by microstrip patch antennas and arrays residing in a cavity, IEEE Trans Antennas Propagat 39 (1991), 1598–1604.
3. J.M. Jin, The finite element method in electromagnetics, Wiley, New York, 1993.
4. L.T. Pillage and R.A. Rohrer, Asymptotic waveform evaluation for timing analysis, IEEE Trans Computer-Aided Design 9 (1990), 352–366.
5. E. Chiprout and M. Nakhla, Asymptotic waveform evaluation and moment matching for interconnect analysis, Kluwer Academic, Boston, MA, 1994.
6. X. Yuan and Z.J. Cendes, A fast method for computing the spectral response of microwave devices over a broad bandwidth, 1993 URSI Radio Sci Meeting, Ann Arbor, MI, 1993, p. 196.
7. M.A. Kolbehdari, M. Srinivasan, M.S. Nakhla, Q.J. Zhang, and R. Achar, Simultaneous time and frequency domain solutions of EM problems using finite element and CFH techniques, IEEE Trans Microwave Theory Tech 44 (1996), 1526–1534.
8. M. Li, Q.J. Zhang, and M.S. Nakhla, Finite difference solution of EM fields by asymptotic waveform techniques, Proc Inst Elect Eng 143 (1996), 512–520.
9. J. Gong and J.L. Volakis, AWE implementation for electromagnetic FEM analysis, Electron Lett 32 (1996), 2216–2217.
10. S.V. Polstyanko, R. Dyczij-Edlinger, and J.F. Lee, Fast frequency sweep technique for the efficient analysis of dielectric waveguides, IEEE Trans Microwave Theory Tech 45 (1997), 1118–1126.
11. J. Zhang and J.M. Jin, Preliminary study of AWE for FEM analysis of scattering problems, Microwave opt Technol Lett 17 (1998), 7–12.
12. X.M. Zhang and J.F. Lee, Application of the AWE method with the 3-D TVFEM to model spectral responses of passive microwave components, IEEE Trans Microwave Theory Tech 46 (1998), 1735–1741.
13. J.E. Bracken, D.K. Sun, and Z.J. Cendes, *S*-domain methods for simultaneous time and frequency characterization of electromag-

TABLE 1 CPU Times for Calculations on Digital Personal Workstation

Problem	No. of Unknowns	AWE Method		Direct Method		Speed-Up
		Freq. Pts.	CPU Time	Freq. Pts.	CPU Time	
Figure 2	1585	600	265.2 s	120	3254.4 s	12.3
Figures 3 and 4	1741	300	254.2 s	60	4012.8 s	15.8

netic devices, IEEE Trans Microwave Theory Tech 46 (1998), 1277–1290.
14. C.J. Reddy, M.D. Deshpande, C.R. Cockrell, and F.B. Beck, Fast RCS computation over a frequency band using method of moments in conjunction with asymptotic waveform evaluation technique, IEEE Trans Antennas propagat 46 (1998), 1229–1233.
15. C.J. Reddy, M.D. Deshpande, C.R. Cockrell, and F.B. Beck, Fast RCS computation over a frequency band using combined FEM/MoM technique with asymptotic waveform evaluation technique (AWE), Electromagn 18 (1998), 613–630.
16. D. Jiao and J.M. Jin, Fast and accurate frequency-sweep calculations using asymptotic waveform evaluation and combined-field integral equation, tech rep CCEM-4-99, University of Illinois, Mar. 1999.
17. F. Ling, D. Jiao, and J.M. Jin, Efficient electromagnetic modeling of microstrip structures in multilayer media, tech rep CCEM-1-99, University of Illinois, Jan. 1999.
18. D.P. Forrai and E.H. Newman, Radiation and scattering from loaded microstrip antennas over a wide bandwidth, tech rep 719493-1, Ohio State University, Sept. 1988.

CCC 0895-2477/99

MICROSTRIP ANTENNA WITH INTEGRATED PHASE SHIFTER

Y. Turki[1] and R. Staraj[1]
[1] Laboratoire d'Electronique, Antennes et Télécommunications
Université de Nice – Sophia Antipolis
CNRS UPRESA 6071
06560 Valbonne, France

Received 5 April 1999

ABSTRACT: *A microwave microstrip probe-fed antenna with an integrated voltage-controlled phase shifter is investigated. The phase shifter used is a microstrip 90° hybrid loaded by two varactor diodes, allowing a 40° phase shift. It is integrated on the antenna due to multilayer technology. Radiation patterns in the E- and H-planes are similar to those obtained with a simple passive patch.* © 1999 John Wiley & Sons, Inc. Microwave Opt Technol Lett 22: 393–394, 1999.

Key words: *microwave; microstrip antennas; antenna arrays; phase shifter*

INTRODUCTION

Printed arrays antennas, used for electronic scanning because of the phase and magnitude control of the signal feeding each radiating element, still suffer from the size of feeding circuits. Many studies have been carried out to compact these arrays, especially with oscillating antennas which allow us to independently control the phase shift of each element of the array. However, the addition of active components substantially damages the radiation pattern, particularly with regard to the cross polarization in the two measured planes.

In this paper, we present a microwave microstrip antenna operating at 4.95 GHz with an integrated voltage-controlled phase shifter. This antenna allows us, in addition to the gain in compactness, to obtain nearly the same radiation pattern as a simple passive microstrip antenna.

ANTENNA DESIGN AND PRINCIPLE

Tarot, Terret, and Coupez [1] obtained a circular polarization by using a 90° microstrip hybrid stacked on a patch. We decided to apply this principle to realize, due to multilayer technology, an integrated phase shifter (Fig. 1).

The phase shifter used is a well-known 90° hybrid, loaded by two varactor diodes [2]. The principle consists of using the printed antenna as the 90° hybrid ground plane. As the antenna is fed by a semirigid coaxial probe, instead of connecting the external conductor of this coaxial probe on the antenna ground plane, we solder it on the antenna itself. The inner conductor of the probe is then connected to the phase shifter input, which will permit us to phase shift the signal before feeding the antenna. The output of the 90° hybrid is then connected to the patch ground plane through the 50 Ω impedance point. As the field under the cavity is well excited, this output becomes the patch feed. To not create a disturbance in the radiation pattern, the external conductor of the probe has to be soldered at the center of the patch where the field is nil. For the same reason, the thickness and permittivity of the phase shifter substrate have to be small. Moreover, it is obvious that the dimensions of the phase shifter have to be smaller than the patch. To reduce the phase shifter dimensions, a high-permittivity substrate or a thin one must be chosen. The second solution has been selected, and the 90° hybrid dimensions have been optimized at 4.98 GHz with the HP Momentum software, on a substrate of thickness 0.381 mm and the same permittivity as the patch substrate. The antenna considered is a 19.5 mm square patch typically working at 4.98 GHz, and is realized on a substrate having a thickness of 0.762 mm and a dielectric constant of 2.2. The diameter of the external conductor of the coaxial probe used is 2.2 mm, and the inner one is 0.5 mm. The varactor diodes are MA4ST563-L120 having a 5–1 pF capacitance swing for a reverse voltage applied from 0 to 20 V. The phase shift obtained between the two ports varies from 0 to 40°, and the insertion loss is constant and close to -0.7 dB. The dc voltage is transmitted with the HF signal to avoid a biasing circuit. Figure 2 shows the impedance locus of the complete antenna when the inverse voltage applied takes the two extremes values 0 and 20 V. The return loss is always < -10

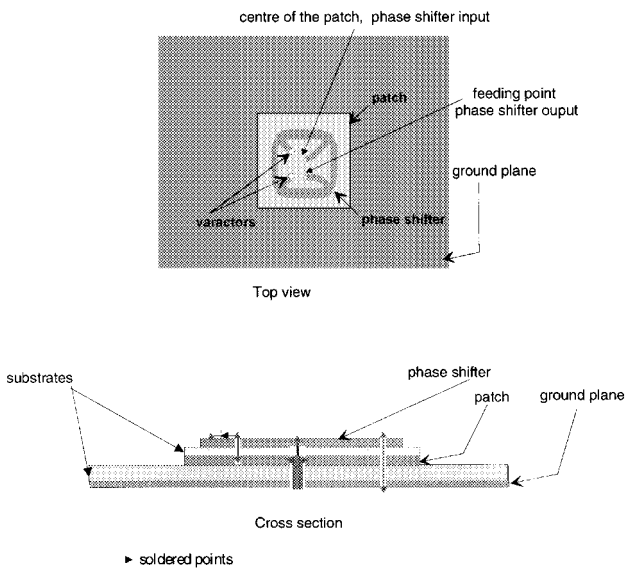

Figure 1 Antenna design